Huang *et al. Journal of Wood Science* (2024) 70:8
https://doi.org/10.1186/s10086-024-02121-9

Journal of Wood Science

REVIEW ARTICLE

Open Access

A rolling shear analysis-based method for determining the apparent stiffness and bending capacity of CLT panel under out-of-plane load

Zirui Huang[1*], Yuling Bian[2] and Chun Ni[3]

Abstract

Most of the currently employed methods, such as Gamma method and shear analogy method, to estimate the bending stiffness and bending capacity of cross-laminated timber (CLT) beams, are computationally extensive. In our previous study, a rolling shear analysis (RSA)-based method, which simplifies the calculation, was developed to determine the shearing capacity of CLT beams. In the present study, the authors expand upon the RSA method to determine the apparent stiffness and bending capacity of 3- and 5-layer CLT beams. By considering the shear deformation of cross layers, simplified formulas to determine the apparent bending stiffness of CLT beam was derived. Two schemes to determine the CLT bending capacity were proposed. One is based on the shear stress analysis, and the other is based on the formula specified in Canadian standard, CSA O86, by replacing the effective stiffness with the apparent stiffness. Test results from the authors and the other researchers were adopted to validate the method. The findings showed that the RSA method, using the apparent stiffness obtained from the proposed method along with the bending capacity formula in CSA O86, can provide a simpler and more reliable estimation of the apparent bending stiffness and bending capacity of CLT beams as compared to the Gamma method and shear analogy method.

Keywords Cross-laminated timber, Apparent stiffness, Moment resistance, Out-of-plane bending, Analyzing mode

Introduction

The heretical structure of cross-laminated timber (CLT) determines that shear weakness must be an inherent property of CLT panels when subjected to out-of-plane bending [1]. As specified in Canadian standard, CSA O86 [2], rolling shear modulus of a CLT board is estimated as 1/160 of the modulus parallel to grain. Hence, the shear deformation in cross layers could be significant, consequently the beam theory based on the Euler–Bernoulli assumption, which stated that the strain on any arbitrary position of a cross section is linearly proportional to the distances from the position to the neutral axis of global bending, cannot be directly applied to the bending problems of CLT beam to predict their bending stiffness and bending capacity. Currently, the most accepted methods for predicting the bending properties of CLT beams [3, 4] are modified from beam theory, such as shear analogy method and Gamma method, etc. These methods assume the cross layer as mechanical joints that carry all the shear deformation of the beam, while the applied load was carried by the parallel layers. The apparent

*Correspondence:
Zirui Huang
huangzirui@seu.edu.cn
[1] School of Civil Engineering, Southeast University, 02 Southeast University Road, Nanjing 211189, China
[2] Wuxi Vocational Institute of Commerce, 809 Qianhu Road, Wuxi 214000, China
[3] Advanced Building Systems, 2665 East Mall, Vancouver V6T 1 W5, Canada

stiffness of the beam was estimated by introducing a connection efficiency parameter (Gamma method) or using Timoshenko beam theory (shear analogy method). The assessment of analytical methods, i.e., shear analogy method and Gamma method for predicting the bending performances of CLT panels was investigated by Christovasilis et al. [5]. They studied the accuracy and the reliability of these methods by comparing the prediction results with the test results, and concluded that all the methods are applicable for determining the bending strength and stiffness whereas have lower reliability for determining the shear performances because of the complicated mechanism of rolling shear.

Extensive studies confirmed that the layup, thickness, and even the saw pattern of CLT boards can significantly influence the performances of rolling shear. Flores et al. [6] studied the rolling shear properties by homogenization and cohesive model on multi-scale beams. The constitutive properties of the model included the information from cell-wall in nanometer-scale and the growing ring in millimeter-scale, whereas the governing equation was obtained by using homogenization technique and was solved by using finite element method. Obviously, this multi-scale model is not applicable for design calculation because it is impossible for the manufactures to provide the material properties on micro scale. Franzonia et al. [7] presented an analytical solution for two-layered beam with interlayer slip and provided an analytical solution for deflection, slip, cross-sectional rotation, and internal forces. In order to assess the CLT panels with regular gaps in cross layers, Ecsedi et al. [8] modeled the CLT panels with gaps as a space frame of beams connected with wooden blocks. A closed-form formulas for predicting the panel's stiffnesses and maximum longitudinal and rolling shear stresses were developed. In general, the methods mentioned above have taken comprehensive effects of rolling shear into consideration, however, they are complicated for design use.

Numerical methods are considered as the most powerful way to deal with the material anisotropy of CLT beams. The literatures on this field are abundant [9–15]. However, because of the difficulties to simulate the complicated damage process, extensive calculations are also need [16]. For this reason, analytical model is still an attractive method for the analysis of CLT beams.

More recently, Huang et al. [17] developed an analytical model to predict the shear capacity of short-span CLT beams. The model takes the cross layer as a continuum joint medium between the parallel layers. CLT bending member is treated as a composite beam that consist of the parallel layers coupled by the joint medium. The simplified formulas to predict the shear capacity of CLT beams were obtained based on the analysis of rolling shear stress. Hence, the model was named as rolling stress analysis-based model (RSA) model. To deal with CLT cross layers as continuum joint medium was firstly reported by Huang et al. [18] when they developed a model to predict the load-carrying capacity of CLT panels loaded with combined bending and compression.

By using RSA method, the present study aims to develop an analytical method to determine the apparent stiffness and the bending capacity of CLT beams. Simplified formulas applicable for design calculations were proposed. The formulas are much simpler than the currently used approaches but without losing accuracy. This paper is arranged as follows. After introduction, the most popular methods accepted by the design standard / manus, i.e., Gamma method, shear analogy method, and the simplified method in CSA O86, were summarized in 'Summary of currently used methods'. The establishment of RSA model used for design purpose to predict the apparent bending stiffness and bending capacity of CLT beams was presented in 'Methods'. Validation of the proposed RSA model was given in 'Validation'; and finally, discussions and conclusions on the use of RSA method were provided in 'Discussions and conclusions'.

Summary of currently used methods

Apparent bending stiffness

Gamma method and shear analogy method are based on the mechanical joint theory which was originally developed for the composite beams connected with fasteners to calculate their apparent stiffness [19]. It was modified for CLT bending problem by imaging the cross layers as continuously distributed fasteners with slip modulus being equal to the modulus of rolling shear [20]. It assumes the load on CLT beam are only carried by the boards oriented in the longitudinal direction, while shear deformations are only occurred in cross layers. A coefficient, γ, was introduced to measure the connection efficiency of cross layer, with $\gamma = 1$ representing completely glued members, and $\gamma = 0$ representing no connection at all. The apparent bending stiffness of CLT beam can be determined by

$$(\mathrm{EI})_{\mathrm{app}} = \sum_{i=1}^{n} \left(E_i I_i + \gamma_i E_i A_i Z_i^2 \right) \tag{1}$$

The connection coefficient, γ, can be determined as follow

$$\gamma_i = \left(1 + \frac{\pi^2 E_i A_i}{L^2} \cdot \frac{t}{G_{\mathrm{R}} b} \right)^{-1} \tag{2}$$

Shear analogy method models CLT panel as two virtual beams, beams A and B, coupled by infinitely rigid web.

They are used to obtain the sum of the moment of inertia and the second moment of area for all the individual layers, respectively. The effective bending stiffness of the CLT beam equals to the summation of the stiffness of beam A and beam B, and is denoted as

$$(\mathrm{EI})_{\mathrm{eff}} = \sum_{i=1}^{n} \left(E_i I_i + E_i A_i Z_i^2 \right) \tag{3}$$

The effective shear stiffness of the beam is determined by

$$(\mathrm{GA})_{\mathrm{eff}} = a^2 \left(\frac{h_1}{2G_1 b} + \sum_{i=2}^{n-1} \frac{h_i}{G_i b_i} + \frac{h_{\mathrm{n}}}{2G_{\mathrm{n}} b} \right)^{-1} \tag{4}$$

The deflection of the beam is calculated referring to Timoshenko beam theory by replacing the bending stiffness, EI, and shear stiffness, GA, with the effective bending stiffness, $(\mathrm{EI})_{\mathrm{eff}}$, and effective shear stiffness, $(\mathrm{GA})_{\mathrm{eff}}$, respectively. For the simply supported CLT beam, the apparent bending stiffness can be shown as Eq. (5).

$$(\mathrm{EI})_{\mathrm{app}} = \frac{(\mathrm{EI})_{\mathrm{eff}}}{1 + 12(\mathrm{EI})_{\mathrm{eff}}/(\mathrm{GA})_{\mathrm{eff}} L^2} \tag{5}$$

Shear analogy method has been employed in Canadian standard CSA O86 [2] to calculate the bending stiffness of CLT beams.

Moment resistance

Gamma method assumes the failure happens if the summation of normal stress on the outmost parallel layer caused by local and global bending reaches its bending strength. The moment of resistance of CLT beam, according to Gamma method, can be given as

$$M_{\mathrm{r}} = \frac{f_b (\mathrm{EI})_{\mathrm{eff}}}{E_{\mathrm{L}} (\gamma_1 Z_1 + 0.5 h_1)} \tag{6}$$

where, h_1 is the thickness of the outer parallel layer.

The method to calculate the moment resistance for CLT beam used in CSA O86 [2] is a simplified method. It was modified from Euler's beam theory for calculating normal stress over the cross-section of the isotropic beams by replacing the bending stiffness with the effective stiffness. The moment resistance is denoted as

$$M_{\mathrm{r}} = \phi \frac{f_b (\mathrm{EI})_{\mathrm{eff}}}{0.5 E_{\mathrm{L}} H} \tag{7}$$

where, H is the depth of CLT beam; $\phi = 0.9$ is the resistance factor. This formula is also adopted by shear analogy method to calculated the moment resistance by replacing the effective stiffness with the associated apparent bending stiffness.

Obviously, the above methods ignored the mechanism of rolling shear. Furthermore, Eqs. (1), (2), and (5) show that the apparent bending stiffness calculated form Gamma method and shear analogy method are reduced with the decrease of squared length of the span of CLT beam. As shown in the following text, the apparent bending stiffness can be significantly lower than the effective stiffness if the span-to-depth ratio is less than 15. This could lead to unacceptable errors for calculating the moment resistance and deformation for CLT beams of small span-to-depth ratio. To overcome the above shortcomings, RSA method was adopted in the present study. The method firstly derived the apparent bending stiffness on the bases of rolling shear analysis, and then provide a simplified formula to determine the bending capacity of CLT beams. The details are presented as follows.

Methods

Rolling shear stress

For simplicity but without losing generality, consider a simply supported 3-layer CLT beam with a concentrated load between the two supports, shown as Fig. 1a. According to the RSA method proposed by Huang et al. [17], the cross layer is deemed as a continuum joint medium while the external load is carried by the parallel layers. Take the segment from the left support to the arbitrary position $x \le l$, which subjected to combined bending and shearing actions (BS segment), into consideration. The forces on the BS segment of a length x can be illustrated as Fig. 1(b), where, x is the distance from the left support to the loading position. Supposing the moduli of elasticity (MOE) of parallel layers and cross layers in longitudinal direction are E_0 and E_{90}, respectively, and the modulus of rolling shear is G_{R}. The rolling shear stress varies against the location, x, has been derived by previous study [17] and can be noted as Eq. (8).

$$\tau(x) = \psi \left(e^{\alpha x} + e^{-\alpha x} \right) + \frac{2\beta}{\alpha^2} V_2 \tag{8}$$

where, V_2 is the shear force carried by the lower parallel layer; α, β, and ψ are parameters independent of the variable x. For 3-layer panel, α is given as

$$\alpha^2 = \frac{G_{\mathrm{R}}}{E_0 t} \left(\frac{2}{A} + \frac{h^2}{2I} \right) \tag{9}$$

while for 5-layer CLT, α is given as

$$\alpha^2 = \frac{G_{\mathrm{R}}}{E_0 t} \left(\frac{1}{A} + \frac{3h^2}{4I} \right) \tag{10}$$

The other two parameters are given as Eqs. (11) and (12).

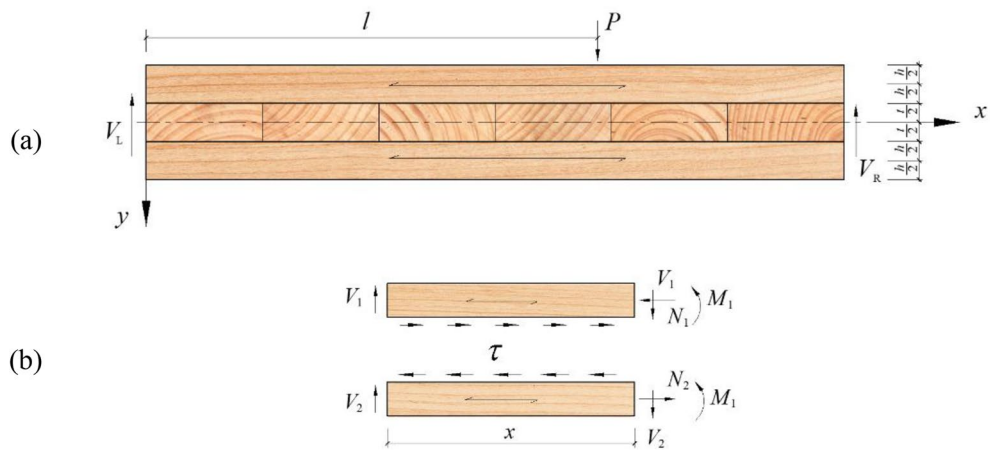

Fig.1 Mechanical model for rolling shear analysis; **a** the simply supported CLT beam with a concentrated load; **b** the internal forces on the parallel layers; where, V_L and V_R are the reaction forces at the left and right support, respectively

$$\beta = \frac{G_R h}{2E_0 It} \tag{11}$$

$$\psi = -\frac{2\beta V_2}{\alpha^2(e^{\alpha l} + e^{-\alpha l})} \tag{12}$$

where, h and t are the thickness of parallel and cross layers, respectively; I is the section moment of inertia of parallel layers; A is the section area of parallel layers. For simplicity, supposing the beam has unit width, hence there must have $I = h^3/12$ and $A = h$. The axial force and the moment carried by the outmost parallel layer can be obtained by the equilibrium conditions, shown as Fig. 1b, which can be expressed as [17]

$$N_2(x) = \int_0^x \tau(x)\,dx = \frac{\psi}{\alpha}\left(e^{\alpha x} - e^{-\alpha x}\right) + \frac{2\beta}{\alpha^2}V_2 x \tag{13}$$

$$M_2(x) = V_2 x - \frac{h}{2}N_2(x) \tag{14}$$

Because the parallel layers have the same thickness, there must have that $V_1 = V_2$, $M_1 = M_2$, and $N_1 = -N_2$. Thus, the axial force and moment on the upper parallel can be obtained.

Apparent bending stiffness

For the simply supported beam shown in Fig. 1, the effective bending stiffness, $(\mathrm{EI})_{\mathrm{eff}}$, can be noted as Eq. (15) if the shear deformation is ignored.

$$(\mathrm{EI})_{\mathrm{eff}} = \sum_{i=1}^{n}(E_i I_i + A_i Z_i) \tag{15}$$

where, E_i is the MOE of each layer. It equals to E_0 for parallel layer while equals to E_{90} for cross layer; I_i and A_i are the moment of inertia and area of each layer, respectively; Z_i is the distance from the center of each layer to the neutral axial of global bending. Assuming the moment-induced deflection is y_{m}, the deflection of the beam at any position must fulfill Eq. (16).

$$(\mathrm{EI})_{\mathrm{eff}}\frac{d^2 y_{\mathrm{m}}}{dx^2} = -M \tag{16}$$

where, M is the moment on the beam. On the other hand, if the deflection caused by shear deformation is considered, the overall deflection of the beam must be the sum of the deflections caused by bending and shearing, i.e., $y = y_s + y_m$. Thus, the deformation of the beam can be expressed as

$$(\mathrm{EI})_{\mathrm{app}}\frac{d^2}{dx^2}\left(y_{\mathrm{s}} + y_{\mathrm{m}}\right) = -M \tag{17}$$

where, $(\mathrm{EI})_{\mathrm{app}}$ is the apparent stiffness of which shear deformation is considered; y_{s} is the deflection caused by shear deformation. Obviously, Eqs. (16) and (17) give the relationship between the effective stiffness and apparent stiffness, shown as Eq. (18).

$$(\mathrm{EI})_{\mathrm{app}} = \frac{(EI)_{\mathrm{eff}}}{1 + y_{\mathrm{s}}''/y_{\mathrm{m}}''} \tag{18}$$

where, $y'' = \frac{d^2 y}{dx^2}$. According to the beam theory [21], the contribution of the axial deformation to the vertical deflection can be ignored, thus, the shear strain of the cross layer can be expressed as Eq. (19).

$$\gamma_R = \frac{dy_s}{dx} \tag{19}$$

where, γ_R is the strain of rolling shear. For the rolling shear stress, τ, the constitutive law yields $\gamma_R = \tau/G_R$, hence we further have

$$\frac{d^2y_s}{dx^2} = \frac{1}{G_R}\frac{d\tau}{dx} \tag{20}$$

Substituting Eq. (8) into Eq. (20) leads to

$$\frac{d^2y_s}{dx^2} = \frac{\alpha\psi}{G_R}\left(e^{\alpha x} - e^{-\alpha x}\right) \tag{21}$$

Substituting Eq. (12) into Eq. (21), and considering $V = 2V_2$ for 3-layer CLT panel, Eq. (21) can be further written as

$$\frac{d^2y_s}{dx^2} = -\frac{2\beta V_2}{\alpha(e^{\alpha x} + e^{-\alpha x})G_R}\left(e^{\alpha x} - e^{-\alpha x}\right) \tag{22}$$

Using Eqs. (16), (18), (20), and, (22), and considering $M = Vx$, and $(e^{\alpha x} + e^{-\alpha x})/\left(e^{\alpha x} - e^{-\alpha x}\right) \to 1$ as x increasing, the relationship between the apparent stiffness and the effective stiffness can be obtained, shown as Eq. (23).

$$(\mathrm{EI})_{\mathrm{app}} = \frac{(EI)_{\mathrm{eff}}}{1 + \frac{\beta(EI)_{\mathrm{eff}}}{\alpha G_R x}} \tag{23}$$

Equation (23) indicates that the apparent stiffness is the function of position, x. It varies along the longitudinal direction from one section to another. Since the amount of the variation is not significant, the apparent stiffness at the loading position, where the maximum deflection occurs, is taken as the apparent stiffness of the beam. Let $x = l$, and substituting Eqs. (9) or (10), and (11) into Eq. (22), yield the apparent stiffness of 3-layer CLT beam and 5-layer CLT beam, shown as Eqs. (24) and (25), respectively.

$$(\mathrm{EI})_{\mathrm{app}} = \frac{(\mathrm{EI})_{\mathrm{eff}}}{1 + \frac{h}{24l}\sqrt{\frac{3E_0 h}{G_R t}}} \tag{24}$$

$$(\mathrm{EI})_{\mathrm{app}} = \frac{(\mathrm{EI})_{\mathrm{eff}}}{1 + \frac{h}{2l}\sqrt{\frac{E_0 h}{10G_R t}}} \tag{25}$$

Usually, the thickness of parallel layers and cross layers are the same. The modulus of rolling shear G_R can be estimated as $E_0/160$ according CSA O86. Therefore, Eqs. (24) and (25) can be further simplify as Eqs. (26) and (27), respectively.

$$(\mathrm{EI})_{\mathrm{app,\ 3\text{-}layer}} = \frac{(\mathrm{EI})_{\mathrm{eff}}}{1 + \frac{\sqrt{30}H}{3L}} \tag{26}$$

$$(\mathrm{EI})_{\mathrm{app,\ 5\text{-}layer}} = \frac{(\mathrm{EI})_{\mathrm{eff}}}{1 + \frac{4H}{5L}} \tag{27}$$

where, H is the depth of CLT panel. For conservation, it can be taken as *3 h* for 3-layer CLT panel and 5 *h* for 5-layer CLT panel; L is the span of CLT beam. Equations (26) and (27) show that the apparent stiffness depends on the span-to-depth ratio, section sizes, and the MOE of material. This finding differs from that of Gamma method and shear analogy method because the apparent stiffness calculated from to these two methods depends on L^2.

In order to illustrate the influence of span-to-depth ratio on the reduction of apparent stiffness of CLT beams, we define the quantity

$$\zeta = \frac{(\mathrm{EI})_{\mathrm{app}}}{(\mathrm{EI})_{\mathrm{eff}}} \tag{28}$$

as the coefficient of stiffness reduction due to rolling shear. For 3-layer and 5-layer, the coefficients can be noted as Eq. (29) and (30), respectively.

$$\varsigma_{\text{3-layer}} = \left(1 + \frac{\sqrt{30}H}{3L}\right)^{-1} \tag{29}$$

$$\varsigma_{\text{5-layer}} = \left(1 + \frac{4H}{5L}\right)^{-1} \tag{30}$$

Figure 2 compares the coefficient of stiffness reduction versus the span-to-depth ratio calculated by RSA method, Gamma method, and shear analogy method. The results of all three methods indicated that the stiffness reduction for 3-layer CLT panels is smaller

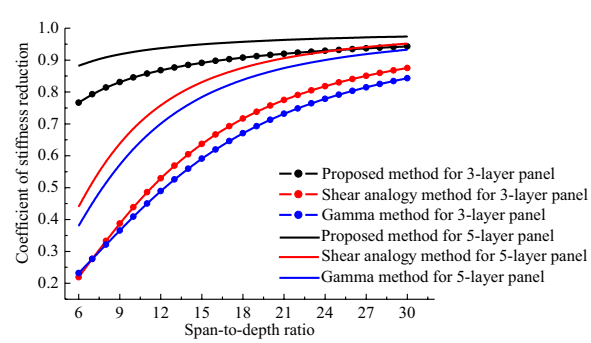

Fig. 2 Comparing of the coefficients of stiffness reduction calculated from RSA method, shear analogy method, and Gamma method

than that for 5-layer CLT panels. Based on the RSA method, the coefficient of stiffness reduction for the RSA method ranged from 0.77 to 0.94 for 3-layer panels and from 0.87 to 0.97 for 5-layer panels, with a change in the span-to-depth ratio between 6 and 30. On the other hand, the Gamma method showed a coefficient of stiffness reduction ranging from 0.23 to 0.83 for 3-layer panels and from 0.38 to 0.92 for 5-layer panels. Similarly, the results for shear analogy method are consistent with RSA and Gamma methods. Figure 2 shows that the apparent stiffness of CLT beams, calculated by both Gamma method and shear analogy method, is significantly lower than the effective stiffness for beams with small span-to-depth ratios. For example, for 5-layer panels with a span-to-depth ratio less than 12, the apparent stiffness decreases by 25% while for 3-layer panels, the decrease is 50%. However, the RSA method shows the apparent stiffness only about 10% lower for 5-layer panels and up to 25% lower for 3-layer panels. For larger span-to-depth ratios, like those greater than 30, the apparent stiffness calculated using all three methods becomes identical for 5-layer panels. In contrast, for 3-layer panels, the RSA method produces results that are approximately 10% higher than those obtained from Gamma method and shear analogy method. These results are similar to those reported earlier by Christovasilis in their research [5], which stated that the shear analogy method underestimates the bending stiffness of softwood and hardwood CLT panels by less than 5% and 25%, respectively. These findings suggest that the RSA method is more accurate in predicting the real bending stiffness of CLT beams compared to Gamma method and shear analogy method.

Moment resistance

It has been confirmed by extensive studies [22–25] that the bending failure of CLT beams are usually caused by the rupture of the outmost parallel layer. Therefore, it is reasonable to establish the failure criterion of CLT beam on the bases of analyzing outmost parallel layer. We firstly take the 3-layer CLT beam into consideration. Assuming parallel layers have the same thickness, the internal forces on the interested section are shown in Fig. 3a. It shows that the moment resistance at the cross section can be noted as

$$M_{\mathrm{r}} = M_1 + M_2 + N(h+t) \tag{31}$$

where, t is the thickness of cross layer; h is the thickness of parallel layers. Let $M_2(l)$, $N_2(l)$, and $V_2(l)$, denote the moment, axial force, and the shear force at the failure section, respectively, the failure condition of the layer can be expressed as

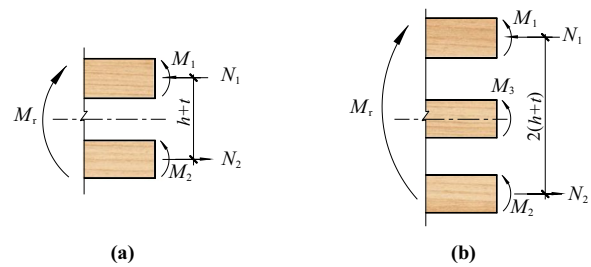

Fig. 3 The moment resistance and the internal forces on the cross section; **a** 3-layer beam; **b** 5-layer beam

$$\frac{N_2(l)}{A_2} + \frac{M_2(l)}{W_2} = f_{\mathrm{b}} \tag{32}$$

where, f_{b} is the bending strength of the lower parallel layer; A_2 and W_2 are the area and the section modulus of the failure cross section, respectively. Using Eqs. (13), (14) and Eq. (32), and considering that the value of item $e^{-\alpha l}$ is much smaller than that of $e^{\alpha l}$ because the bending member usually has large span, the vertical force on the failure cross section can be obtained, as shown in Eq. (33).

$$V_2 = \frac{f_b}{\frac{2\beta}{\alpha^2}\left(\frac{1}{A_2} - \frac{h}{2W_2}\right)\left(l - \frac{1}{\alpha}\right) + \frac{l}{W_2}} \tag{33}$$

Therefore, the axial force and the moment at failure section can be obtained by using Eqs. (33), (13), and (14), shown as Eqs. (34) and (35), respectively.

$$N_2(l) = \frac{2\beta}{\alpha^2}\left(l - \frac{1}{\alpha}\right)V_2 \tag{34}$$

$$M_2 = V_2 l - \frac{1}{2}hN_2 \tag{35}$$

The moment resistance of the 3-layer CLT beam can be obtained by using Eqs. (31), (33), and (35), as shown in Eqs. (36).

$$M_{\mathrm{r,3\text{-}layer}} = 2M_2 + N_2(h+t) \tag{36}$$

For 5-layer CLT beam, the local moment carried by the middle parallel layer is $M_3 = h\int_0^l \tau(x)\,dx = N_2 h = 2M_2$, as shown in Fig. 3 (b). Thus, the moment resistance of the 5-layer CLT beam can be calculated as

$$M_{\mathrm{r,5\text{-}layer}} = 4M_2 + 2N_2(h+t) \tag{37}$$

Equations (36) and (37) can be further expressed as Eqs. (38) and (39) by using Eqs. (36), (37), and (32).

$$M_{\mathrm{r,\,3\text{-}layer}} = \frac{[\lambda(2+\eta)l + \xi(h+t)]f_{\mathrm{b}}}{\left[\frac{2\beta}{\alpha^2}\left(\frac{1}{A_2} - \frac{h}{2W_2}\right)\left(l - \frac{1}{\alpha}\right) + \frac{l}{W_2}\right]} \tag{38}$$

$$M_{\mathrm{r,\,5\text{-}layer}} = \frac{[\lambda(3+2\eta)l + 2\xi(h+t)]f_{\mathrm{b}}}{\left[\frac{2\beta}{\alpha^2}\left(\frac{1}{A_2} - \frac{h}{2W_2}\right)\left(l - \frac{1}{\alpha}\right) + \frac{l}{W_2}\right]} \tag{39}$$

where, the coefficients are denoted as

$$\lambda = 1 - \frac{\beta h}{\alpha^2}\left(1 - \frac{1}{\alpha l}\right) \tag{40}$$

$$\xi = \frac{2\beta}{\alpha^2}\left(l - \frac{1}{\alpha}\right) \tag{41}$$

Equations (38) and (39) are complicated and are not user friendly for design calculation. It is perhaps more convenient to use the method specified in CSA O86 by replacing the effective stiffness with the apparent stiffness shown in Eqs. (42) and (43) for 3-layer CLT beam and 5-layer CLT beam, respectively. Thus, the formula to determine the bending resistances of 3-layer and 5-layer CLT beams can be noted as Eqs. (42) and (43), respectively.

$$M_{\mathrm{r,\,3\text{-}layer}} = \frac{f_b(\mathrm{EI})_{\mathrm{eff}}}{0.5E_0H} \cdot \left(1 + \frac{\sqrt{30}H}{3L}\right)^{-1} \tag{42}$$

$$M_{\mathrm{r,\,5\text{-}layer}} = \frac{f_b(\mathrm{EI})_{\mathrm{eff}}}{0.5E_0H} \cdot \left(1 + \frac{4H}{5L}\right)^{-1} \tag{43}$$

If we let $\phi = \left(1 + \frac{\sqrt{30}H}{3L}\right)^{-1}$ for 3-layer CLT beam and $\phi = \left(1 + \frac{4H}{5L}\right)^{-1}$ for 5-layer CLT beam, Eqs. (42) and (43) have the same form as Eq. (7) specified on Canadian standard CSA O86 to determine the bending capacity of CLT beams. However, it is important to note that the definition of ϕ in CSA O86 pertains to reliability considerations, which differs from the concept of stiffness reduction coefficient proposed in this study. As demonstrated in 'Apparent bending stiffness' that coefficient ϕ varies from 0.85 to 0.94 for 3-layer CLT panel, while from 0.94 to 0.97 for 5-layer CLT panel, as the span-to-depth ratio varies from 12 to 30. This happens to be largely consistent with the value specified in CSA O86.

Validation

In order to validate the proposed model, specimens tested by the authors and the other researchers [26–28] were adopted as the samples for predicting the apparent stiffness and bending capacity. The material properties and the specimen dimensions are presented in Table 1. The specimens named as SPF-3 and SPF-5 were test by the authors. The laminations that were used to make the CLT panels came from Canada and glued by a Chinese Company. The MOE and the strength of bending strength of the laminations were obtained from 4-point bending test in accordance with the ASTM standard D 198 [29]. In total 9 specimens were tested to determine the MOE and the bending strength, respectively. The mean values of the tested results are shown in Table 1. The mean value of the MOE of bending is 8360 MPa with the variable coefficient of 11.71, and the bending strength is 31.02 MPa with the variable coefficient of 5.49. The specimens tested by the other researchers were originally used to determine the bending strength of the CLT laminations by using Gamma method or shear analogy method. In the following validation calculations, the bending strength is used as the input to calculate the maximum load of CLT beams.

Table 1 Mechanical properties and dimensions of the validation specimens

References	Specimens	Number of layers	Material properties (MPa)	Dimensions (mm)
Test by the authors	SPF-3/3000	3	$E_0 = 8360, f_b = 31.02$	$b = 400, h = 35, t = 35, L = 3300, a = 1000$
	SPF-5/3000	5	$E_0 = 8360, f_b = 31.02$	$b = 400, h = 35, t = 35, L = 3300, a = 1000$
He [26]	CLT-S/4825	5	$E_0 = 10766.510766.5, f_b = 24.91$	$b = 305, h = 35, t = 35, L = 4825, a = 1887.5$
Navaratnam [27]	CL3/105/2100	3	$E_0 = 8000, f_b = 26.61$	$b = 520, h = 35, t = 35, L = 2100, a = 682.5$
	CL3/105/2940	3	$E_0 = 8000, f_b = 23.41$	$b = 520, h = 35, t = 35, L = 2940, a = 1102.5$
	CL5/145/2900	5	$E_0 = 8000, f_b = 28.67$	$b = 520, h = 35, t = 20, L = 2900, a = 942.5$
	CL5/145/4020	5	$E_0 = 8000, f_b = 26.84$	$b = 520, h = 35, t = 20, L = 4020, a = 1575$
Sikora [28]	B-3-20/1440	3	$E_0 = 8160, f_b = 37.71$	$b = 270, h = 20, t = 20, L = 1440, a = 540$
	B-3-24/1296	3	$E_0 = 8160, f_b = 35.55$	$b = 288, h = 24, t = 24, L = 1296, a = 432$
	B-3-40/2880	3	$E_0 = 8160, f_b = 25.14$	$b = 584, h = 40, t = 40, L = 2880, a = 1080$
	B-5-20/2400	5	$E_0 = 8160, f_b = 33.62$	$b = 576, h = 20, t = 20, L = 2400, a = 900$

Table 2 presents the apparent bending stiffnesses obtained from the test and the prediction by using RSA method, Gamma method, and shear analogy method. The effective stiffnesses are also included. It is evident that the RSA method gives the most accurate prediction for all test specimens. Except for specimen CL3/105/2100, differences between the prediction and the test results fall within ± 20%. Gamma method and Shear analogy method yield similar prediction on apparent bending stiffness, however, the differences between the prediction and test results are larger than RSA method.

It should be noted from Table 2 that for the first seven specimens, the apparent bending stiffness from the tests are greater than the effective stiffness. As the apparent stiffness must be smaller than the effective stiffness due to the shear deformation. Therefore, these apparent stiffnesses must be overestimated in tests.

Table 3 compares bending capacities of the specimens obtained by testing with those determined by RSA method, Gamma method, shear analogy method, and the method in CSA O86. The values in RSA-1 column were calculated by using Eq. (36) or Eq. (37), and those in RSA-2 column were calculated by using Eq. (42) or Eq. (43). The discrepancies between the prediction and the test results are also presented in Table 3. Discrepancies that are greater than ± 20% are highlighted in grey. It was found that for the specimens CLT-S/4825 and CLT3/105/2100, the discrepancies are greater than ± 20%. For specimen CL3/105/2940, only the proposed method, i.e., RSA-2, gives the closest prediction with a discrepancy of -10.96%, whereas the predictions from the other methods significantly deviated from test results.

Furthermore, it is evident, according to Table 3, that the predictions obtained using Eq. (31) and CSA O86 are highly comparable. With the exception of unreliable

Table 2 Comparing the apparent stiffness obtained by prediction with that by testing

Specimens	Span-to-depth ratio	Test (kN·m^2)	Effective stiffness (kN·m^2)	Proposed method (kN·m^2)	Differences (%)	Gamma (kN·m^2)	Differences	Shear analogy (kN·m^2)	Differences (%)
SPF-3/3000	28.57	3.865	3.130	3.100	−19.79	2.674	−30.82	2.755	−28.72
SPF-5/3000	17.14	14.158	11.876	11.630	−17.86	10.098	−28.68	10.056	−28.97
CLT-S/4825	27.57	15.781	11.663	11.496	−18.29	10.751	−30.87	11.049	−29.99
CL3/105/2100	20.00	4.57	3.894	3.836	−27.15	2.777	−39.23	2.935	−35.78
CL3/105/2940	28.00	4.75	3.894	3.852	−15.71	3.212	−32.38	3.329	−29.92
CL5/145/2900	20.00	10.70	9.276	8.989	−15.99	8.231	−23.07	8.404	−20.16
CL5/145/4020	27.72	9.73	9.276	9.067	−6.81	8.691	−10.68	8.810	−9.64
B-3-20/1440	24.00	0.369	0.385	0.380	2.89	0.2996	−18.81	0.3131	−15.15
B-3-24/1296	18.00	0.664	0.709	0.697	4.95	0.4756	−28.37	0.5060	−23.80
B-3-40/2880	24.00	6.361	6.659	6.576	3.38	5.184	−18.50	5.419	−14.81
B-5-20/2400	24.0	3.139	3.115	3.064	−2.39	2.805	−10.64	2.890	−7.90

Table 3 Comparing the bending capacity obtained by prediction and that by testing

Specimens	Test (kN·m^2)	RSA-1 (kN·m^2)/Error		RSA-2 (kN·m^2)/Error (%)		Gamma (kN·m^2)/ Error (%)		Shear analogy (kN·m^2)/Error		CSA O86 (kN·m^2)/Error (%)	
SPF-3/3300	23.18	23.23	0.22	27.56	18.90	22.28	−3.88	20.65	−10.91	23.31	0.56
SPF-5/3300	52.07	52.29	0.42	42.43	−18.51	51.64	−6.47	44.81	−13.84	53.65	3.03
CLT-S/4825	41.35	30.40	−26.48	26.28	−36.44	30.29	−26.75	29.22	−29.33	30.98	−25.08
CL3/105/2100	32.35	24.30	−24.88	25.13	−22.32	22.08	−31.75	18.60	−42.50	24.51	−24.23
CL3/105/2940	28.65	21.47	−25.06	25.51	−10.96	20.39	−28.83	18.56	−35.22	21.57	−24.71
CL5/145/2900	49.19	44.43	−9.68	44.72	−9.09	44.62	−9.29	41.54	−16.77	45.97	−6.55
CL5/145/4020	45.44	41.61	−8.43	44.35	−2.40	41.80	−8.01	38.99	−14.19	43.03	−5.30
B-3-20/1440	5.88	5.85	−0.51	6.70	13.95	5.46	−7.14	4.82	−18.03	5.89	0.17
B-3-24/1296	8.52	8.44	−0.94	8.47	−0.59	7.52	−11.74	6.12	−28.17	8.53	0.12
B-3-40/2880	33.94	33.76	−0.53	38.66	13.91	31.53	−7.10	27.83	−18.00	33.98	0.41
B-5-20/2400	25.78	25.25	−2.06	21.45	−16.80	25.10	−2.64	23.99	−6.94	25.79	0.04

data highlighted in gray, both RSA method and CSA O86, i.e., Eqs. (31) and (7), provide reasonable estimations for the bending capacity of CLT beams. The accuracy of the Gamma method surpasses that of the shear analogy method. Therefore, it can be inferred that the RSA and CSA O86 methods are both straightforward and dependable in determining the bending capacity of CLT beams.

Discussions and conclusions

In general, the RSA method yields larger predictions of apparent stiffness for CLT beams compared to those predicted by the Gamma method and shear analogy method. However, as the span-to-depth ratio increases, the predicted bending stiffness from these three methods tend to convergence. Comparing to the effective bending stiffness which ignores the effect of rolling shear, when the span-to-depth ratio of CLT beam less than 12, the prediction apparent stiffness is up to 80% lower for 5-layer beam and 60% lower for 3-layer beam. Test results indicated that RSA method gives more reliable prediction for bending stiffness. Therefore, it is recommended that RSA method can be used to determine the apparent stiffness.

RSA method takes the cross layer of CLT beam as the continuum joint media that couples the parallels as a composite beam. By replacing the constrains of the cross layers with the rolling shear stress for the parallel layers, RSA method converts the analysis of the parallel layer of CLT beam to the problem of elastic-foundation beam. Bending capacity was obtained by treating the rolling shear stress as an applied load on parallel layer. The limitation of this method is that the vertical forces at the end of cross layers are ignored, which could lead to the predicted rolling shear stress deviating from the real case, especially for more than 3-layer CLT beams. Therefore, RSA method may lead to great errors in predicting the bending capacity of the CLT beams with more than five layers. However, because RSA method yields good prediction of apparent bending stiffness, Eqs. (42) and (43) are recommended to determine the bending capacity of CLT beams.

Abbreviations

A_i	Section area of *i*th layer
a	The distance between the centers of outmost layers
b	Width of CLT beam
E_i	MOE of *i*th layer in longitudinal direction
E_L	MOE in longitudinal direction of CLT beam
E_0	MOE parallel to grain of a panel
E_{90}	MOE perpendicular to grain of a panel
f_b	The bending strength of outer layer
G_R	Modulus of rolling shear
G_i	Shear modulus of *i*th layer; for cross layer, it equals to G_R
h_i	The thickness of *i*th layer
H	The depth of CLT beam
I_i	The section moment of inertia of *i*th layer
L	Span of CLT beam
l	Length of bending−shearing segment
M_i	Bending moment on *i*th layer
N_i	Axial force on *i*th layer
V_i	Shear force on *i*th layer
t	Thickness of cross layer
Z_i	The distance from the center if *i*th layer to the neutral axis of global bending
α,β	Distribution parameters of the rolling shear stress
γ_i	Coefficient of connection efficiency for *i*-th layer
γ_R	Rolling shear strain
ψ	Magnitude of rolling shear stress distribution
ϕ	Factor of moment resistance
$(EI)_{eff}$	Effective bending stiffness
$(EI)_{app}$	Apparent bending stiffness
$(GA)_{eff}$	Effective shear modulus
CLT	Cross-laminated timber
RSA	Rolling Shear Analysis
BS	Bending and Shearing
MOE	Modulus of Elasticity
SPF	Spruce-Pine-Fir
CSA	Canadian Standard Association

Acknowledgements

The authors would like to thank Prof. Dongsheng Huang of Nanjing Forestry University, China, for his gently guidance during the whole program; Prof. Zhongfan Chen from Southeast University and Dr. Yurong Shen from Nanjing Forestry University, China, for supporting of the related data collection and analysis provided for some of the work reported herein; Zhongjia Low Carbon Co. Ltd. at Ningbo, China, for their contributions of manufacturing the cross-laminated timber used in the tests.

Author contributions

ZH accomplished all the theoretical analysis and the manuscript writing work. YB supported some of the data analysis of the tests. CN provided theoretical and technical support of the whole research work presented in the manuscript. All the authors have read and approved the final manuscript.

Funding

Funding for the research was provided by the National Natural Science Foundation of China (Grant No. 52208234), through the young scholar scientific research program implemented in Southeast University.

Availability of data and materials

Not applicable.

Declarations

Competing interests

The authors declare no competing interests.

Received: 16 July 2023 Accepted: 11 January 2024
Published online: 24 January 2024

References

1. Perret O, Douthe C, Lebeée A, Sab K (2011) A shear criterion for the buckling analysis of CLT walls. Eng Struct 211:110344
2. CSA O86-4 (2017) Engineering design in wood reprinted in Jun. Canadian Standard Association, SCA Group, Ontario
3. Canadian Wood Council (2017) Wood design manual Ontario Ottawa
4. Karacabeyli E, Doulas B (2011) CLT Handbook. FPInnovations, Quebec
5. Christovasilis IP, Brunetti M, Follesa M, Nocetti M, Vassallo M (2016) Evaluation of the mechanical properties of cross laminated timber with elementary beam theories. Constr Build Mater 122:202–213
6. Flores EIS, Saavedra K, Hinojosa J, Chandra Y, Das R (2016) Multi-scale modelling of rolling shear failure in cross-laminated timber structures by homogenization and cohesive zone models. Int J Solids Struct 81:219–232

7. Franzonia L, Lebée A, Lyon F, Forêt G (2018) Closed-form solutions for predicting the thick elastic plate behavior of CLT and timber panels with gaps. Eng Struct 164:290–304
8. Ecsedi I, Baksa A (2016) Analytical solution for layered composite beams with partial shear interaction based on Timoshenko beam theory. Eng Struct 155:107–117
9. Acter ST, Serrano E, Bader TK (2021) Numerical modelling of wood under combined loading of compression perpendicular to the grain and rolling shear. Eng Struct 244:112800
10. Silva JVF, Pereira MCDM, Silva MFF, Molina JC (2023) Experimental and numerical analysis of specimen configurations for cross laminated timber on rolling shear stiffness and strength response. Eng Struct 284:115973
11. Oñate A, Fernándea J, Saavedra K (2023) Numerical simulation on the influence of delamination on the critical buckling load of CLT panels. Eng Struct 286:116209
12. Perret O, Lebée A, Douthe C, Sab K (2018) Experimental determination of the equivalent-layer shear stiffness of CLT through four-point bending of sandwich beams. Constr Build Mater 186:1132–1143
13. Hematabadi H, Madhoushi M, Khazaeyan A, Ebrahimi G, Hindman D, Loferski J (2020) Bending and shear properties of cross-laminated timber panels made of poplar (*Populus alba*). Constr Build Mater 265:120326
14. Li X, Ashraf M, Subhani M, Kremer P, Kafle B, Ghabraie K (2020) Experimental and numerical study on bending properties of heterogeneous lamella layups in cross laminated timber using Australian Radiata Pine. Constr Build Mater 247:118525
15. Marjanovic M, Markovic N, Damnjanovic E, Cvetkovic R (2020) Three-dimensional stress analysis and design of cross-laminated timber panels using full-layerwise-theory-based finite element method. Thin-wall Struct 157:107156
16. Li M, Füssl J, Lukacevic M, Martin CM, Eberhardsteiner J (2019) Bending strength predictions of cross-laminated timber plates subjected to concentrated loading using 3D finite-element-based limit analysis approaches. Compos Struct 220:912–925
17. Huang Z, Huang D, Chui Y-H, Chen Z (2023) A layered beam-based model for analyzing the stress of rolling shear for the cross-laminated timber panels under out-of-plane bending. Eng Struct 289:116290
18. Huang Z, Huang D, Chui Y-H, Shen Y, Daneshvar H, Sheng B, Chen Z (2022) Modeling of cross laminated-timber (CLT) panels loaded with combined out-of-plane bending and compression. Eng Struct 250:113335
19. EN 1995: 2008–06 (2016) Eurocode 5: Design of timber structures-Part 1–1: General-Common rules and rules for buildings. European Committee for Standardization, Asociación Española de Normalización y Certificación. https://www.astm.org/cgi-bin/resolver.cgi?3PC+UNE+UNE_UNE-EN_1995-1-1+en-US
20. Gagnon S, Pirvu C (2011) CLT Handbook. FPInnovation, Special Publication, Quebec
21. Timoshenko S (1940) Strength of materials, Part I: elementary theory and problems, 2nd edn. D. Van Nostrand C. Inc., New York
22. Crovella P, Simth W, Bartczak J (2019) Experimental verification of shear analogy approach to predict bending stiffness for softwood and hardwood cross-laminated timber panels. Constr Build Mater 229:116895
23. Shen Y, Huang Z, Daneshvar H, Chui Y-H, Huang D (2023) Experimental study of CLT panels under combined out-of-plane bending and compression. Eng Struct 275:115262
24. Daniel FL, Violeta GA, María P, Guillermo IG (2022) Cross laminated timber (CLT) manufacture with European oak recovered from demolition: structure properties and no-destructive evaluation. Constr Build Mater 339:127635
25. Hojat H, Mehrab M, Abolghasem K, Ghanbar E (2021) Structural performance of hybrid Poplar Beech cross-laminated-timber (CLT). J Build Eng 44:102959
26. He M, Sun X, Li Z (2018) Bending and compressive properties of cross-laminated timber (CLT) panels made from Canadian hemlock. Constr Build Mater 185:175–183
27. Navaratnam S, Christopher PB, Ngo T, Le TV (2020) Bending and shear performance of Australia Radiata pine cross-laminated timber. Constr Build Mater 232:117215
28. Sikora SK, McPolin DO, Harte AM (2016) Effects of the thickness of cross-laminated timber (CLT) panels made from Irish Sitka spruce on mechanical performance in bending and shear. Constr Build Mater 116:141–150
29. ASTM D198-5 (2015) Standard test methods of static tests of lumber in structural sizes. American Society for Testing and Materials (ASTM), West Conshohocken

Publisher's Note